ADVANCES IN PHYSICS: X
2021, VOL. 6, NO. 1, 1889402
https://doi.org/10.1080/23746149.2021.1889402

Taylor & Francis
Taylor & Francis Group

REVIEWS

OPEN ACCESS Check for updates

# Nonlinear wave mixing in lithium niobate thin film

Yuanlin Zheng [a,b] and Xianfeng Chen [a,b,c,d]

[a]State Key Laboratory of Advanced Optical Communication Systems and Networks, School of Physics and Astronomy, Shanghai Jiao Tong University, Shanghai China; [b]Shanghai Research Center for Quantum Sciences, Shanghai China; [c]Jinan Institute of Quantum Technology, Jinan China; [d]Collaborative Innovation Center of Light Manipulation and Applications, Shandong Normal University, Jinan China

**ABSTRACT**

Lithium niobate on insulator (LNOI), by taking advantage of versatile properties of lithium niobate (LN) and a large refractive index contrast, provides an ideal on-chip platform for studying a broad range of optical effects as well as developing various superior photonic devices. It is a game-changer technology for traditional LN-based applications. Especially, with recent advances in the fabrication of high-quality micro-/nano-structures and devices on the LNOI platform, LN-based integrated photonics has been propelled to new heights. In this review, we summarize the latest research advances in lithium niobate thin film (LNTF), with a special focus on nonlinear wave mixing and their photonics applications. Different types of second- and third-order nonlinear processes in LNOI micro- and nano-structures are reviewed, including nonlinear frequency conversion, frequency comb generation and supercontinuum generation. Furthermore, perspectives for photonic integrated circuits (PICs) on the LNOI platform in nonlinear optics regime are predicted.

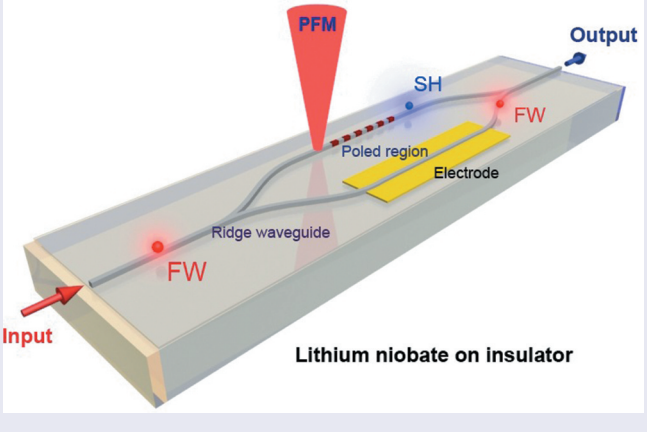


**ARTICLE HISTORY**
Received 30 November 2020
Accepted 6 February 2021

**KEYWORDS**
Lithium niobate on insulator; lithium niobate thin film; photonic integrated circuit; nonlinear wave mixing; frequency conversion

**CONTACT** Xianfeng Chen xfchen@sjtu.edu.cn State Key Laboratory of Advanced Optical Communication Systems and Networks, School of Physics and Astronomy, Shanghai Jiao Tong University, Shanghai 200240, China

**PACS CODES** 42.65.–k Nonlinear optics; 42.82.–m Integrated optics; 42.70.Mp Nonlinear optical crystals; 42.65.Ky Frequency conversion.

## 1. Introduction

Lithium niobate ($LiNbO_3$, LN) is a significant ferroelectric crystal with exceptional optical properties. Often dubbed as the 'silicon of photonics,' it possesses versatile properties including wide transparency window, relatively high refractive index, large electric-optical coefficient, strong second-order nonlinearity, as well as acousto-optic effect and piezoelectricity. Moreover, its ferroelectric domain can be engineered to achieve quasi-phase matching (QPM) for efficient nonlinear or electro-optic wave mixing. It has been the workhorse of modern optics and optical communication for decades, serving as essential long-haul optical modulators in telecommunication networks [1], frequency converters in nonlinear optics [2,3], single-photon sources in quantum optics [4,5], as well as surface acoustic wave actuators in phononics [6,7]. Each of these properties has been well explored and pushed to the limit after so many years of intensive study and development. Yet, one particular drawback, that is, lack of dense integration capability, had been hindering its ultimate performance and applications.

Recently, the lithium niobate-on-insulator (LNOI) technology has brought a new life to the old material. It facilitates the resurgence of integrated photonics based on the material, arousing significant attention over these few years [8–11]. Because the LNOI technology has brought to the new platform a full capability of on-planar integration, bridging the final gap between LN multifunctionality and fully integrated photonics. By the ion slice and wafer-bonding technology (or smart cut technology), single-crystalline lithium niobate thin film (LNTF) of several hundred nanometer thick (typically 300–900 nm) with different crystalline orientation can be sliced off and bonded to a silica buffering layer on a wafer substrate (which can be bulk LN, silicon, quartz, etc.). Detailed fabrication procedures have already been well summarized [8]. Nowadays, LNOI wafers of six-inch sizes have been commercially available, and larger size wafers can be expected readily obtainable within few years. The downstream of large-scale production can be envisioned in the short future [12], and the cost will also drop significantly.

The research in this field, invoked by the mature development of the LNOI technology and the capability of fabrication of high-quality LNOI photonic structures, has made significant progress over the past few years. The fabrication of micro/nanostructures in LNTF, like femtosecond laser writing with focused ion beam milling, argon ion milling, reactive ion etching, induced coupled plasmon and chemo-mechanical polishing, can be referred to Refs. [13–15], where technical details have been given. The propagation loss of LNOI nanowaveguides has been reduced to an ultimate low level (less than 0.03 dB/cm in nanophotonic waveguides [16,17], or equivalently, the quality factor in microresonators higher than $10^7$ [18]),

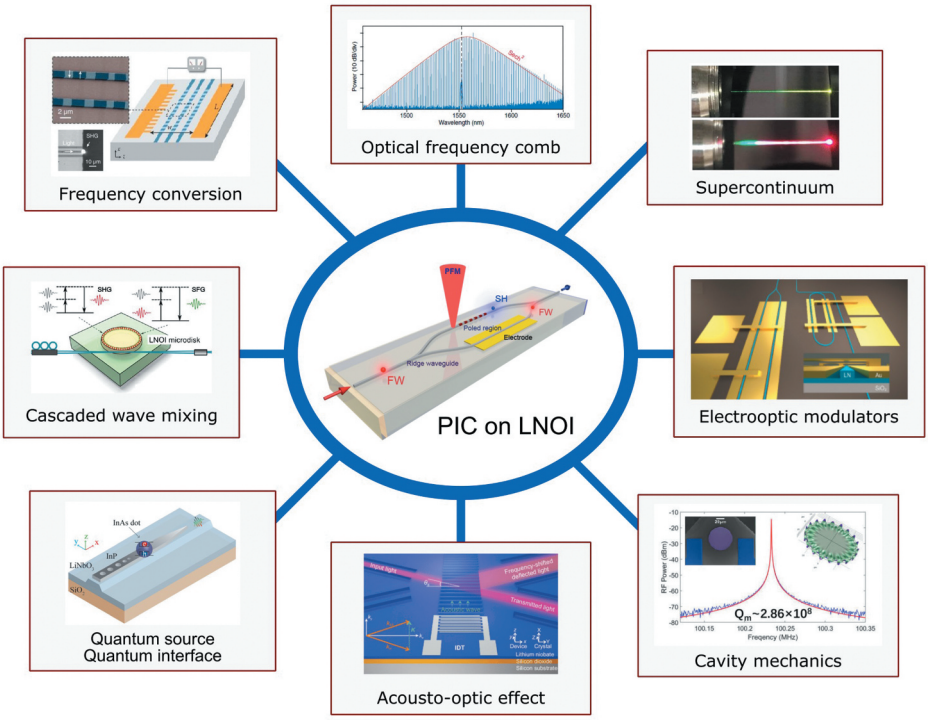


**Figure 1.** Schematic of LNOI for integrated photonics applications.

approaching the limit of the material absorption. Besides multifunctional properties of LN, the LNOI possesses a high refractive index contrast with respect to the buffering silica layer ($\Delta n \sim 0.7$), offering over an order of magnitude improvement in optical confinement. The bent radii of LNOI nanowaveguides (or photonic wires) can be as short as several micrometers – the key step for dense integration. Integration offers not only reduced footprints, confining light in small volumes also dramatically enhances its interaction with matter, and through nonlinear wave mixing processes creates new frequencies. The impact of the interrupt technology is remarkably profound. Just like silicon-on-insulator (SOI) for silicon integrated photonics, LNOI has the great potential to be revolutionary for LN-based photonics. And with the exceptional nonlinearity of LN, it has also opened up a new territory for integrated linear and nonlinear photonics. Important applications of LNOI for optical, electro-optic, acousto-optic, quantum, and optomechanic devices and applications are schematically shown in Figure 1.

The potential of LNOI, like SOI, shows no boundary. In the very recent years, remarkable advances have been made in integrated optics on the LNOI platform. Linear optics on the LNOI platform has been well summarized and several pertinent reviews have been given [9,19–21]. In this review, we only focus on the current progresses in the nonlinear optics aspect of

LNTF or the LNOI platform. We restrict the scope to nonlinear wave mixing processes and their applications for nonlinear integrated photonics, both point-to-point and in perspectives. We aim for a comprehensive treatment that incorporates the state-of-the-art experiments and points the way toward perspective applications.

This review is organized as follows: In Section 2, we focus on nonlinear wave mixing regarding second-order nonlinear ($\chi^{(2)}$) effects in LNTF, with an emphasis on the most classical types of processes. Cascaded quadratic ($\chi^{(2)}:\chi^{(2)}$) processes will also be included. In Section 3, third-order nonlinear effects in LNTF are reviewed, such as optical frequency comb and supercontinuum generation. And in Section 4 we summarize the outlook and future challenges for LNOI-based photonics.

## 2. Second-order nonlinear effects in LNTF

The primary building blocks for integrated nonlinear photonics applications, like their linear counterparts, are also based on the same structures such as micro-/nano-waveguides, whispering-gallery-mode (WGM) microcavities and photonic crystal (PhC) micro-/nanocavities, in which the enhanced light-matter interaction takes place. Nonlinear wave mixings greatly benefit from the strong light confinement of LN nanowaveguides and its strong second-order nonlinearity ($\chi^{(2)}$). Especially, the dispersion in LNOI nanowaveguides can be well designed and controlled, thus flexible phase matching (PM) schemes can be feasible and achievable. This has led to a branch of fascinating phenomena in nonlinear optics with ultrahigh efficiency or ultralow input power, including second-harmonic generation (SHG), sum frequency generation (SFG), difference frequency generation (DFG), optical parametric oscillation/amplification (OPO/OPA), spontaneous parametric down conversion (SPDC), etc. These parametric processes are popular methods for wavelength conversion, coherent light sources and photon-pair generation.

For nonlinear processes, achieving high conversion efficiency is a primary goal, where the realization of PM is vital. LNOI has provided more degrees of freedom to realize such goal. We firstly discuss the most classic second-order process, i.e. SHG, in different schemes.

### 2.1 SHG with high conversion efficiency

SHG, or frequency doubling, is the phenomenon where an input fundamental wave generates a new wave with twice its optical frequency in a nonlinear medium. SHG can be modeled based on the coupled mode theory. The wave equation under the small-signal and slowly varying amplitude approximation reads $dA_2/dz = \left(i\omega_2^2 d_{\text{eff}}/2k_2c^2\right)A_1^2 e^{i\Delta kz}$, where $A$

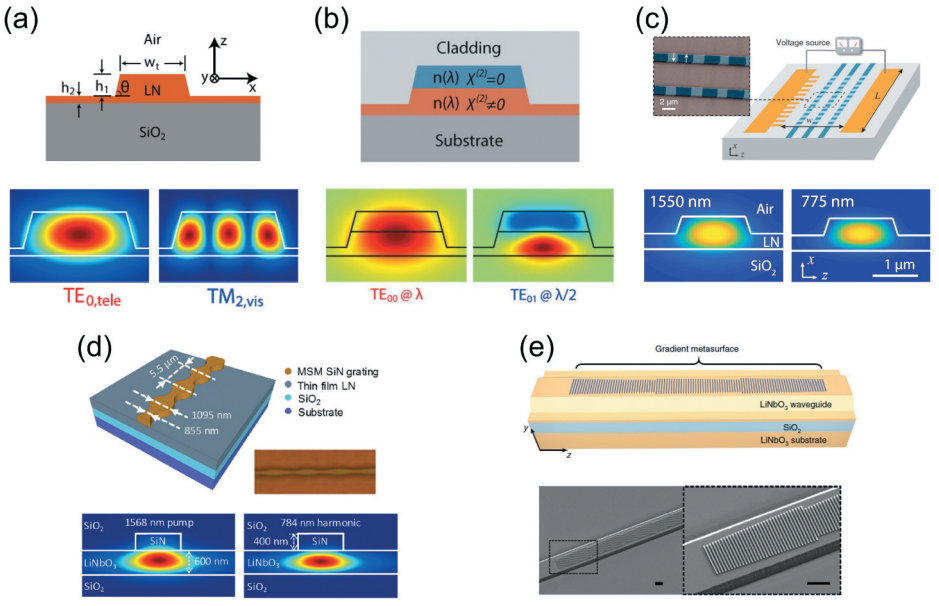


**Figure 2.** Different PM schemes for SHG in LNOI nanowaveguides. (a) Intermodal PM between low-order FW mode and high-order SH mode. Adapted with permission from [22] © The Optical Society. (b) Semi-nonlinear structure for breaking the spatial symmetry of the nonlinearity. Adapted with permission from [23] © Wiley-VCH GmbH. (c) QPM by periodic domain reversal. Adapted with permission from [24] © The Optical Society. (d) Mode-shape modulation periodically altering the FW amplitude. Adapted with permission from [31] © AIP Publishing LLC. (e) Metasurface assisted PM, which provides a unidirectional effective wavevector 32] Copyright © The Author(s)

is the mode amplitude, $\omega$ is the angular frequency, $d_{\text{eff}}$ is the effective nonlinear coefficient, $k$ is the wavevector, $\Delta k = k_2 - 2k_1$ is the wavevector mismatch, $z$ is the interaction length, and $c$ is the speed of light. The subscripts $1, 2$ represent fundamental wave (FW) and second harmonic (SH), respectively. The wave mixing in waveguides requires additional consideration of waveguide dispersion and mode overlapping, which requires case-to-case calculation. From the wave equation, one can see that the critical PM condition can be realized in different ways, which includes: (i) Intermodal PM for $\Delta k = k_2 - 2k_1 = 0$ (Birefringence PM is a very restrictive condition and not directly accessible in LNOI waveguides); (ii) QPM, that is, the reciprocal vector ($G$) of periodic modulation ($\Lambda$) of second-order susceptibility $\chi^{(2)}$ compensates the wavevector mismatch when $G = 2\pi/\Lambda = \Delta k$; and (iii) The periodic modulation of the FW amplitude itself, where $A_1$ varies periodically. This is typically achieved by periodically modulating the waveguide cross-section. These schemes have all been carried out on the LNOI platform.

Intermodal PM is achieved by engineering the mode dispersion of the nonlinear waveguide at the cost of a reduced mode overlap between the low-order FW mode and a higher-order SH mode (their effective refractive

indices are the same), thereby compromising the nonlinear efficiency. However, the overall performance can still be significant in nanowaveguides and doubly resonant microcavities. In Figure 2(a), intermodal PM is adopted to achieve the momentum conservation condition between fundamental TE mode in the telecom band and third-order TM mode in the visible [22]. And with the thermo-optic birefringence of LN, flexible PM spectral tuning was also demonstrated in a wide span of 60 nm. Besides, a wise concept of semi-nonlinear waveguide structure [23] was proposed and demonstrated by breaking the spatial symmetry of the optical nonlinearity of the waveguide, thus circumventing the difficult poling procedure, see Figure 2(b). The intermodal PM is achieved between fundamental TE and second-order TE modes, which is forbidden in homogeneous waveguides because the mode overlapping integral is zero. The idea has the guiding meaning to other quadratic nonlinear platforms as well.

The popular QPM is a versatile scheme to compensate the phase mismatch of nonlinear interactions in ferroelectric crystals like LN, which can take advantage of the largest nonlinear coefficient tenser element. Due to a stronger dispersion, QPM grating period is smaller than its bulk counterpart, which imposes some difficulty in such implementation in LNTF. Although electrical poling technique is mature in bulk ferroelectric materials, the work on LNTF still requires more effort. In 2018, Cheng Wang *et al.* reported directly fabricate QPM by electrical poling technique in *x*-cut LNOI nanowaveguides, and achieved a record high efficiency of 2600% $W^{-1}cm^{-2}$ [24], see also Figure 2(c). This is over an order of magnitude improvement than the record high proton exchanged LN waveguides. Domain reversal of LNTF was realized using direct electrical poling, the same as the poling of LN. Other than direct poling, calligraphic poling methods are appealing for complex structures, if more components are to be integrated on the same chip. Attracting approaches also involves electron beam writing, femtosecond laser direct writing, and atomic force microscope, which has been achieved at bulk surfaces [25–28] and is also applicable for LNTF. For example, Zhenzhong Hao *et al.* have demonstrated

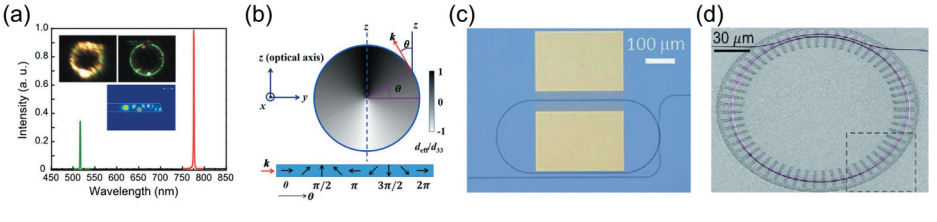


**Figure 3.** SHG and PM schemes in LNOI WGM microresonators. (a) Intermodal PM. Adapted with permission from [77] © The Optical Society. (b) cyclic QPM. The variations of  of a TE-polarized mode. Adapted with permission from [38] © The American Physical Society. Direct QPM in (c) racetrack and (d) circular microrings . Adapted with permission from [41, 42] © The Optical Society

domain engineering in LNTF microdisks by using piezoresponse force microscopy (PFM) [29].

Before the demonstration of periodical poling in LNTF, periodically grooved waveguides were used to achieve QPM in nanowaveguides. Effective QPM condition was realized through the periodical modulation of the waveguide width, but at a cost of high scattering loss. Normalized SHG efficiency was 6.8%$W^{-1}cm^{-2}$ [30]. An alternative way relies on a sinusoidal width modulation of the rib-loaded waveguides on top of the LNLF [31], see also Figure 2(d). The overall conversion efficiency is relatively low, ~1%$W^{-1}cm^{-2}$. Another novel scheme of metasurface-assisted PM [32], as proposed by Cheng Wang *et al.*, has demonstrated the suppression of backward conversion, see also Figure 2(e). One of the main differences between gradient metasurfaces and periodically poled domains is that gradient metasurfaces provide a unidirectional effective wavevector, thus enabling one-way energy transfer from the FW to SH wave. However, the fabrication is high-demanding and the length is limited (dozens of um). Metasurfaces enhanced SHG in LNOI via Mie-type resonance was also reported [33]. However, due to their thin dimensions, the overall conversion efficiency is still really low, typically less than $10^{-5}$ using pulsed pump. This will not be discussed in detail in this review. The research can be found in related literature [34,35].

Other than conversion efficiency (a main figure of merit), the conversion bandwidth is another consideration. LNOI nanowaveguides with short lengths can provide high conversion efficiency while maintaining a large bandwidth. Whereas bulk (and conventional waveguide) periodically poled lithium niobate (PPLN), whose length is on the order of cm, typically has a 1-nm and 1-degree tolerance in respective bandwidth and temperature at the telecommunication bands. Highly spectrally tunable PM capability can be realized by varying the temperature with a measured tuning slope of 0.84 nm/K for a telecom pump, an order of magnitude larger than that in LN bulk [22]. Other than temperature tuning, Licheng Ge *et al.* also demonstrated a broadband QPM scheme by leveraging the weak chromatic

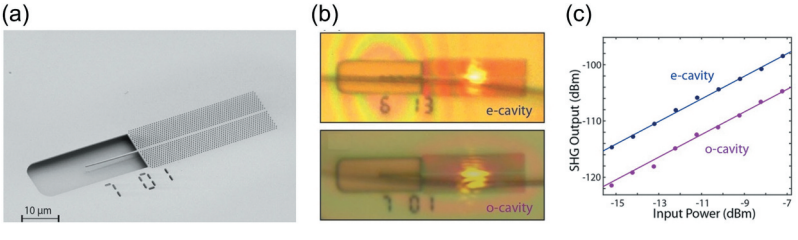


**Figure 4.** SHG in LNOI PhC nanocavity. (a) SEM image of a fabricated 2D LN PhC slab cavity. (b) Optical microscopy images of the PhC cavity pumped by e- and o-polarized light. (c) Generated SH wave intensity with respect to the input power. Adapted with permission from [48] © Wiley-VCH GmbH.

dispersion of MgO:PPLN thin film in the telecommunication band [36]. Such properties of LNOI nanowaveguides are useful in achieving both stable frequency converters (insensitive to wavelength shift or temperature fluctuation) and wideband tunable coherent light based on frequency conversion.

By proper PM techniques, the harmonic conversion efficiency in LNOI photonic waveguides has been improved dramatically in a few years. Higher efficiency can be achieved in microresonators where enhancement takes place in high-quality WGM cavities. In contrast to waveguides, both PM and double resonance conditions should be satisfied to achieve efficient SHG, which are much more stringent.

The intermodal PM leverages the equal effective refractive index of lower-order FW (typically fundamental order) and that of a higher-order SH one, or equivalently, the SH azimuthal order is twice of the FW, i.e. $m_{\mathrm{SH}} = 2m_{\mathrm{FW}}$. The condition can be met in microresonators occasionally in experiment but difficult to determine by the structure design and fabrication. By using a 30-um LNOI microdisk, Shijie Liu *et al.* was able to observe both SHG and the consequent cascaded SFG [37], as shown in Figure 3(a). Thus, an effective cascaded third-harmonic generation (THG) was possible even the WGM cavity had a moderate quality (Q) factor of $10^5$. Due to a weak mode overlapping, the SHG conversion efficiency is relatively low, only at an order of $10^{-6}/\mathrm{mW}$.

Innovatively, Jiantian Lin *et al.* revealed a unique broadband QPM mechanism in *x*-cut LNOI microdisks [38]. In a *x* -cut LNOI microdisk as the wave traveling around the circumference, the TE-polarized mode experiences a rotating crystal orientation [Figure 3(b)], i.e. cyclic variation of the effective nonlinear coefficient $d_{\mathrm{eff}}$, analogy to the effect of periodic domain inversion in a PPLN crystal. This method demonstrates another way for achieving efficient SHG in LNOI microcavities without periodical poling. And with TE pumping, the largest second-order nonlinear coefficient $d_{33}$ can be utilized. SHG and cascaded THG with normalized conversion efficiencies up to 9.9%/mW and $1.05\%/\mathrm{mW}^2$ were demonstrated in the LNOI microdisk with a Q factor close to $10^7$ at ~1550 nm.

To further boost the efficiency, direct QPM in LNOI microresonators is the key solution. But it is also highly demanding in fabrication. The QPM microdisk resonator can be fabricated from periodically poled LNTF or by PFM technique [39,40]. In 2019, two research groups independently demonstrated ultrahigh efficient SHG in microring resonators by precise and uniform periodical poling in *x*-cut and *z*-cut LNTF micro-racetrack and microring resonators [41,42], see also Figure 3(c) and 3(d). The QPM grating was inscribed by direct electrical poling, similar to that in PPLN fabrication. Each of the methods requires precision micro-/nanofabrication

techniques for structure geometries and domain patterning. An ultrahigh conversion efficiency of over $2 \times 10^5\%/\mathrm{W}$ was demonstrated. Improved from their previous work, Juanjuan Lu *et al.* recently reported a record high conversion efficiency of 5,000,000%/W SHG efficiency in a similar scheme, reaching a single-photon nonlinear anharmonicity approaching 1% [43]. With further improvement, demonstration of giant nonlinearity in the few-photon and single-photon level can thus be envisioned, which is highly desired in quantum applications.

The PhC cavity on the LNOI platform is also a promising candidate for efficient nonlinear optics, because they have the smallest mode volume of all, typically on the scale of $(\lambda/n)^3$. PhC cavities have the ability to realize nonlinearity at few-photon level, promising for the ultimate goal of single-photon nonlinearity. LNOI PhC structures, such as defect, nanobeam, and slab cavities, have been reported [44–48]. Figure 4 shows SHG in a two-dimensional LNOI PhC slab nanocavity [48]. The Q factor of the resonators has reached over $10^5$ with an SHG conversion efficiency of $0.078\%\mathrm{W}^{-1}$. The polarization-dependent cavity modes can also enable to probe the anisotropy of nonlinear optical phenomena. Although the efficiency is relatively low to date, the device can be optimized by appropriate design. Leveraging the small mode volume and high Q factors of the nanocavities, highly efficient nonlinearity in few photon or even single photon can be envisioned, which is highly promising in up-conversion detection of single photons, as well as other quantum effects.

### 2.2 Other second-order nonlinear processes

Other classical second-order nonlinear wave mixing processes that have been investigated in LNTF include, but not limit to, SFG, DFG, OPO, OPA, and SPDC. We will not discuss these one by one, but summarize them all in this subsection.

Demonstration of efficient SFG has the application to upconvert low-frequency weak light or single photons, highly useful in infrared signal detection. The first SFG in LNOI microdisks shows an efficiency of $1.4 \times 10^{-7}\mathrm{mW}^{-1}$ through intermodal PM [49]. The Q factors are larger than $3 \times 10^5$ in both fundamental and SFG wavelengths. Our group has also demonstrated SFG via intermodal PM with an efficiency of $2.22 \times 10^{-6}\mathrm{mW}^{-1}$ in an LNOI microdisk with a Q factor of $1.8 \times 10^5$ [50]. SFG in LNOI microresonators with higher conversion efficiency is to be demonstrated using QPM, which should be close to that of SHG. In periodically poled LNTF, broadband SFG using $d_{33}$ was observed on the condition of simultaneous QPM and group velocity matching [51]. The measured QPM bandwidth is about 15.5 nm for a 4-cm long LNTF sample

at the telecommunication band. SFG is also highly useful in quantum interfaces, connecting single photons in the telecommunication bands ('flying qubits') with atomic ensemble-based quantum memories in the near-infrared (NIR) regime. Up-conversion of single photons in LNOI nanowaveguides is exciting. Although one can expect an ultrahigh conversion efficiency, the problem of waveguide coupling should be solved before practical demonstration is done. It is also the mechanism for which efficient microwave-to-optical conversion can be achieved [52]. This has not been realized using LNTF. However, several similar demonstrations on the LNOI platform utilizes acousto-optic effect to shift the optical frequency driven by microwave signal [53,54].

The DFG process is widely used for mid-infrared light sources, IR/NIR spectroscopy and THz generation. Theoretically, the process is similar with OPA and OPO. OPA is appealing in on-chip optical amplification, as well as microwave photonics. Because OPA in $\chi^{(2)}$ nonlinear waveguides are more compact and possesses lower noise as compared to erbium-doped fiber amplifiers or semiconductor optical amplifiers. OPA on the LNOI can be an important tool for signal amplification and regeneration in telecommunication systems, featuring high gain and suppressed noise [55,56]. A net gain of 11.8 dB and an extinction ratio of 14.9 dB was achieved with only 2.4-pJ picosecond pulsed pump in an 8-mm long LNOI nanowaveguides [56]. OPO based on quadratic nonlinearity in LNOI microresonators is yet to be demonstrated. A. W. Bruch *et al*. has realized low-threshold parametric oscillation employing phase-matched AlN microring resonators [57]. The on-chip OPO conversion reached 17% with mW-level output power. Building an on-chip OPO in LNOI would have several immediate applications if the conversion efficiencies are high. For example, by nanometer QPM gratings, mirrorless OPO can be achieved [58,59], as well as backward harmonic generation.

SPDC splits one single photon into two (energy and momentum conservation), thus generating entangled photons. SPDC has been widely utilized in conventional proton-exchanged and titanium-indiffused LN waveguides as quantum light sources [60]. SPDC in *x*-cut LNOI microdisks has demonstrated a wide bandwidth of about 400 nm in the telecommunication band [61], showing significantly improved performance beyond conventional methods. Recently demonstrated in LNOI nanowaveguides, Jie Zhao *et al*. has reported a bright quantum source at the telecommunication band with a pair flux of $11.4 \times 10^6$pairs/s, an ultrahigh CAR (coincidence to accidental ratio) over 67,000, visibility better than 99%, and $g_H^{(2)}(0)$ less than 0.025 at sub-mW pump level [62]. The shallow etched ridge waveguide was fabricated using 300-nm thick MgO-doped *x*-cut LNTF, and the QPM period was 2.8 μm due to a strong dispersion. The

device has a length of only 5 mm, yet the overall performance of the quantum source is significantly higher than those achieved in conventional PPLN waveguides or other material platforms. Shortly after, Zhaohui Ma *et al.* demonstrated ultrabright quantum photon sources on an LNOI chip at a high rate of 36.3 MHz and $g_H^{(2)}(0)$ of 0.097 at only 13.4 μW pump power [63]. A record high CAR of 14,682 ± 4427 was achieved at 210-nW on-chip pump power. They utilized a triply resonant *z*-cut PPLN microring resonator on the LNOI platform. The radius of the microring is 55 μm, and the QPM period was 3.85 μm. The footprint of the device is far smaller than that of LNOI nanowaveguides. The work marks orders of magnitude improvement over the state of the art. With sub-micrometer poling in LNTF [64], it is possible to generate counter-propagating photons pairs [65], which is favored due to its narrow spectral bandwidth characteristics.

### 2.3 Cascading quadratic processes

Complex wave mixing processes contain richer physics and are also more powerful than a single one. A typical example is the cascading process. LN has a moderate third-order coefficient $\chi^{(3)}$, however, the cascading of quadratic ($\chi^{(2)} : \chi^{(2)}$) processes can mimic an efficient third-order nonlinearity. Since second-order susceptibilities are several orders of magnitude larger than third-order ones, the effective third-order susceptibility can be much larger than the intrinsic one. The various PM schemes also provide flexible ways for the implementation of cascaded optical nonlinearities in LNTF.

One direct cascading process involves SHG and consequent SFG to generate third harmonic waves. This can be observed in WGM microresonators with intermodal PM [37]. Other reported cascading effects in LNOI microresonators include simultaneous generation of four-wave mixing (FWM) and stimulated Raman scattering (SRS) in LNOI microring resonators [66] and coupled LNOI microdisks mediated by SHG [67]. However, due to a wide wavelength spanning and different dispersions for sub-processes, the matching condition for this type of cascading can be hard to access. Our group has recently demonstrated effective FWM, i.e. cascaded SHG and DFG (cSHG/DFG), in LNOI microdisk resonators [68]. The advantage is that their wavevector mismatches are close and can be compensated simultaneously or in a wide bandwidth. It is also worth to mention that the effective $\chi^{(3)}$ through $\chi^{(2)} : \chi^{(2)}$ cascading can greatly decrease the threshold of comb generation or supercontinuum if the dispersion of microresonators is properly designed. Direct comb generation and supercontinuum in nanowaveguides can even be possible through continuous wave pumping.

Cascaded quadratic effects are also a main mechanism for high-order harmonic generation (HHG). In 2017, D. D. Hickstein *et al.* reported on up

to 13th harmonic generation in chirped PPLN waveguides on micrometer thick LNOI chips via infrared femtosecond laser pumping [69]. The total conversion efficiency of the harmonics is 10%. It is also appealing to achieve HHG in LNTF nanowaveguides, and the conversion efficiency can be further enhanced.

Electro-optic (EO) effect in crystals essentially arises from their second-order susceptibility. Cascading of EO effect and nonlinear wave mixing has appealing applications in electrically controlled nonlinear photonics. Because the EO coupling has the advantage of fast response and integration, as compared to wavelength and temperature tuning methods [70]. Moreover, the implementation of EO effect and nonlinear wave mixing heralds the realization of quantum sources of complex entangled states of light that can be dynamically tuned via EO effect.

## 3. Third-order nonlinear effects in LNTF

Lithium niobate has a moderate third-order coefficient, direct THG in LN does not show much advantage over other materials, especially when compared with $\chi^{(2)}:\chi^{(2)}$ cascading. Thus, few attempts to demonstrate pure THG in LNTF have been reported. However, through the enhancement resulting from strong confinement and low waveguide loss, LNTF can still sustain efficient third-order wave mixing processes. This is proven by the demonstration of optical frequency comb (OFC) generation in microrings and supercontinuum generation (SCG) in nanowaveguides. Both the processes involve significant spectral broadening of the original pump beam via nonlinear wave mixing, like FWM and nonlinear phase modulation. These devices, i.e. on-chip wide bandwidth coherent light sources, could lead to new opportunities for LNOI applications.

### 3.1. Optical frequency comb generation

OFC or microcomb sources generated from soliton formation in Kerr nonlinear microresonators have been intensively studied. The integrated comb sources are particularly appealing for applications such as metrology, spectroscopy, parallel communication and ranging [71–74]. Only until recently has frequency comb formation be realized in LNOI microring resonators when they reached high-quality factors of $10^6$.

Although all materials possess third-order nonlinearity, frequency comb generation in $\chi^{(2)}$ nonlinear cavities have the potential to achieve direct $f-2f$ self-referencing. This simplified configuration, without off-chip frequency doubling, improves the efficiency and stabilization of the microcomb generator, an advantage over $\chi^{(3)}$ nonlinear cavities. To date,

Kerr soliton combs spanning over 700 nm have already been realized in LNOI microresonators [75], although the utilized nonlinearity is still the third-order one. Mode-locked Kerr soliton comb was later demonstrated [76,77]. Figure 5 shows the experimental results of mode-locked Kerr soliton OFC generation in LNOI microring resonators [76]. The photorefractive effect enables the LN soliton mode-locking process to self-start. Besides, the LNOI microresonator can be switched to soliton states from both directional detuning, an advance over other high-Q resonators on thermo-optic effect. SHG was also observed simultaneously, therefore, one further step towards direct comb self-referencing. OFC generation in LN resonators differs from Kerr cavities in that both second- and third-order nonlinearity simultaneously present towards on-chip self-referenced frequency-comb sources. Scientists are pursuing the goal for LNOI-based microcombs to achieve octave spanning frequency comb and simultaneous on-chip $f-2f$ locking. Broad soliton microcombs in LNTF microring resonators with a spectral span up to 4/5 octave have recently been demonstrated [78], a step closer to this goal. The potential of LNOI microresonators in this configuration is thus profound and exciting.

Until now, OFC and SCG processes have been demonstrated on different material platforms, including $SiO_2$, $Si_3N_4$ and AlN [79], most of which depend on third-order nonlinearity for broadening. While at present broadbandwidth OFC and SCG on the LNOI are still based on $\chi^{(3)}$, there are attempts to exploit hybrid $\chi^{(2)}$ and $\chi^{(3)}$ nonlinearities or only $\chi^{(2)}$ nonlinearity. Not only $\chi^{(2)}$ coefficient is orders of magnitude larger, but also SHG facilitates $f-2f$ self-referencing simultaneously during generation.

The microcomb research also has profound impact on quantum optics, with wide bandwidth photon pair sources integrated on chip,

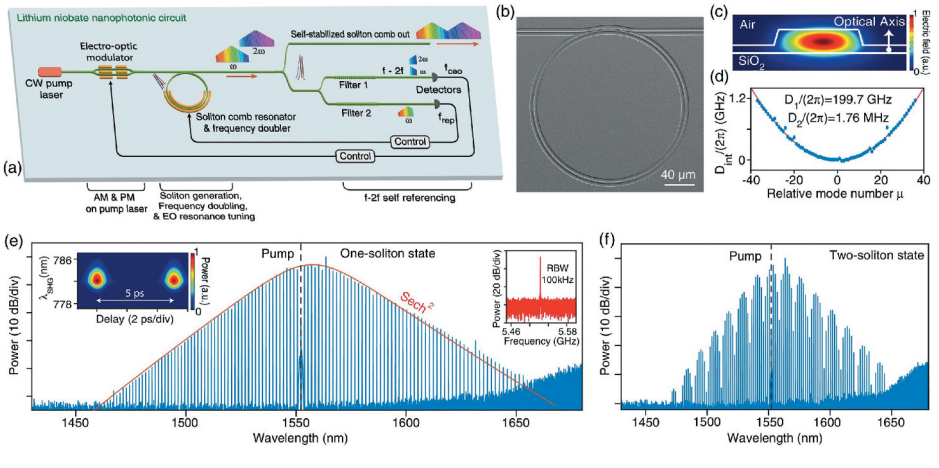


**Figure 5.** Lithium niobate microring resonator and mode-locked Kerr solitons. Adapted with permission from [79] © The Optical Society.

quantum interface for telecommunication and storage. Because 'quantum frequency combs' (operating at the single-photon level) can store and process a large amount of information in the spectral-temporal quantum modes [80]. Besides, it is also worth noticing that a novel EO frequency comb in LNOI microresonators has already been demonstrated via direct EO modulation [81], which is essentially the same with second-order susceptibility in the optical region. The EO comb spacing or repetition rate can be tuned to integer times of the free spectral range (FSR) of the microresonator. The EO comb features a straightforward, simplified mechanism and thus improved reliability.

### 3.2. Supercontinuum generation

The process of SCG involves drastic spectral broadening when intense ultrashort pulses propagate in a nonlinear medium. The physical mechanisms behind SCG include a collection of nonlinear processes, such as modulation instability, self-/cross-phase modulation, SRS and FWM. It provides a way to make coherent ultrawide bandwidth laser sources or white light lasers. SCG, especially in PhC fibers, has been covered in detail by previous reviews [82]. Chip-scale SCG is highly desired for integrated supercontinuum sources for spectroscopy and other on-chip applications. Given that both second- and third-order nonlinearities are simultaneously present, octave spanning SCG and subsequent SHG can allow for on-chip $f-2f$ interferometry. To efficiently generate supercontinuum, accessing anomalous dispersion regime is critical, which requires optimized dispersion engineering.

Several experiments of SCG in LNOI nanowaveguides have been reported [83,84]. Figure 6(a) shows an experimental over 1.5 octave-spanning SCG in LNOI nanowaveguides. The waveguide has a dimension of 1.75um × 0.6um × 10mm, and is pumped by a femtosecond laser (1560 nm, 200 fs, 80 MHz) with an estimated peak power of 4.0 kW inside the waveguide. The numerical modeling can be performed using the generalized nonlinear Schrodinger equation (GNLSE), analogy to the case in

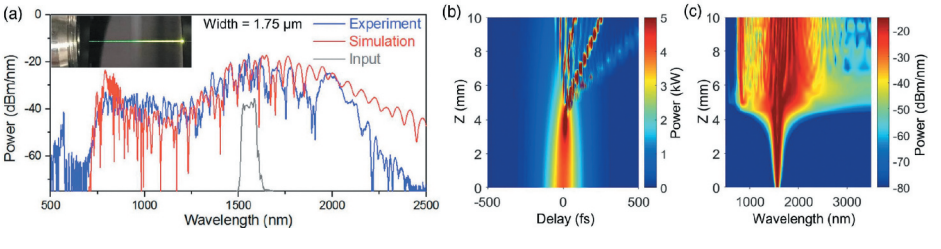


Figure 6. Octave-spanning SCG in LNOI nanowaveguides pumped by NIR femtosecond laser. Adapted with permission from [83] © The Optical Society.

optical fibers, whose theory has been well investigated and established over the past decades. Figure 6(b) and 6(c) respectively, correspond to the calculated temporal and spectral evolution of the incident pulse with respect to position in the waveguide. The simulation and experiment results show that the significant spectral broadening occurs shortly after the soliton fission length of 4.5 mm, shorter than that in PhC fibers or $SiO_2$ waveguides. SHG also takes place during the SCG process, but is phase mismatched. Thus, later investigation of SCG in PPLNOI nanowaveguides may be considered [85].

In addition, there are other nonlinear phenomena in LNTF but are not included in the previous paragraphs due to the space limit. They are Raman lasing [86] and acousto-optics effects [87]. LN with large electromechanical transduction efficiency can be used in acousto-optic coupling for Brillouin integrated photonics. For instance, integrated nonreciprocal devices leveraging Brillouin or acousto-optics in LNTF will become a new frontier.

## 4. Perspectives and conclusion

Over the years, LNTF integrated photonics has enabled remarkable advances in the miniaturization and enhancement of on-chip nonlinear devices. Thanks to its multifunctional properties, strong light confinement and flexibility of device design, the LNTF provides a versatile platform for investigating light-matter interactions in a broad range of research areas. The emerging and potential applications have inspired a drastic increase in the interest of LNTF and LNOI devices for core components of the on-chip systems, chip-scale RF photonics, nonlinear optics, and quantum photonics. This will include applications in frequency metrology, optical to microwave links, single-photon level interactions and large-scale quantum frequency processing. Despite great ongoing progress in nonlinear optics on the LNOI platform, there are much more progresses to be witnessed and much more work to be done.

As of the nonlinear photonics applications, the ultimate goal is to realize 100% (or close to 100%) conversion efficiency and single-photon nonlinearity. The recent work has demonstrated such giant single-photon nonlinearity, showing significant potential in realizing this goal [43,63]. Although the reported nonlinear devices showed ultrahigh normalized efficiency, the overall efficiency is far away from unity. Periodic domain reversal techniques are vital for QPM in LNOI films, and sub-micro domain poling for backward QPM, such as backward SHG [88] and mirrorless OPO [89], is still a challenge. Poling of LNTF with a period of 747 nm was reported by optimized bipolar preconditioning [64], which may also apply to shorter period poling. And poled LNTF even with periods down to 200 nm has also been successfully demonstrated using the PFM method [29]. Backward QPM scheme is thus accessible in LNTF. Backward SHG has the advantage

of separating fundamental and harmonic waves, and backward SPDC generating counter-propagating photon pairs with ultranarrow spectral bandwidth. The scheme is favored especially when the down-converted photon pairs are frequency degenerated.

Wide bandwidth cascaded $\chi^{(2)}:\chi^{(2)}$ nonlinearities for coherent light sources of OFC and SCG can be foreseen. The former has been studied in bulk LN microresonators [90]. By leveraging cascaded $\chi^{(2)}:\chi^{(2)}$ nonlinearities and dispersion management, OFC and SCG at low input intensities can be achieved, which is inaccessible in conventional structures. Cascaded two-stage SPDC via $\chi^{(2)}:\chi^{(2)}$ nonlinearity can generate high-dimensional entangled photon states, such as three-photon states. Cascaded EO effect and nonlinear processes are also worth to study, which provide a manner to electrically control nonlinear processes at fast speeds. This may be beneficial for optical signal processing. The enhanced EO and nonlinearities in LNTF also provides a great platform for investigation of new phenomena in synthetic dimensions [91–93], through which synthetic lattices can be formed in either microresonator or waveguide geometries.

LNOI will become an irreplaceable platform for next-generation integrated photonics, opening new doors to micro- and nano-photonics both in the linear and nonlinear regimes. The trend is to incorporate more optical elements on the sample LNOI chip, such as lasers, EO modulators, microcomb, nonlinear converters, to realized real multifunctional PIC chips. Heterogeneous integration of LNTF and other strong $\chi^{(3)}$ nonlinear materials for advanced nonlinear applications, such as the integration of quantum dots, silicon circuits and III–V semiconductors, will also be a new frontier. Nevertheless, the integrated of laser sources (via rare-earth ion doping) and detectors (based on heterogeneous structures) remains the largest obstacle for full integration on a single chip. Active components of on-chip laser sources on LNOI have recently been demonstrated using erbium-doped lithium niobate microcavities [94,95], which also shows direct possibility to achieve optical amplification in LNOI waveguides. Direct electrical pumping is more favored, but requires much more efforts. Heterogeneous integration of photodetectors using has also been reported [96]. Together with the multifunction of LN, full integration for photon generation, manipulation and detection can be envisioned.

In conclusion, recent advances in nonlinear photonics in LNTF were reviewed. LNOI has risen to the forefront of chip-scale nonlinear photonics, benefiting from the enhanced light-matter interaction due to strong confinement of LNOI nanowaveguides and large nonlinearity of LN. We gave a brief overview, as well as perspective, of nonlinear processes based on the LNOI platform. Tremendous new opportunities exist for innovative approaches that leverage versatile properties of LN. The role of LNTF in the developing of

integrated linear and nonlinear photonics is to exponentially grow.

## Disclosure statement

No potential conflict of interest was reported by the authors.

## Funding

This work was supported by National Natural Science Foundation of China (NSFC) [12074252, 62022058, 11734011]; the National Key R&D Program of China [2018YFA0306301, 2017YFA0303701]; Shanghai Municipal Science and Technology Major Project [2019SHZDZX01-ZX06]; Shanghai Rising-Star Program [20QA1405400]; and Shandong Quancheng Scholarship [00242019024].

## ORCID

Yuanlin Zheng http://orcid.org/0000-0003-4442-1176
Xianfeng Chen http://orcid.org/0000-0002-7574-2047

## References

[1] Wooten EL, Kissa KM, Yi-Yan A, et al. A review of lithium niobate modulators for fiber-optic communications systems. IEEE J Sel Top Quantum Electron. 2000;6:69–82.
[2] Lim EJ, Fejer MM, Byer RL. Second-harmonic generation of green light in periodically poled planar lithium niobate waveguide. Electron Lett. 1989;25:174–175.
[3] Myers LE, Eckardt RC, Fejer MM, et al. Quasi-phase-matched optical parametric oscillators in bulk periodically poled $LiNbO_3$. J Opt Soc Am B. 1995;12:2102–2116.
[4] Caspani L, Xiong C, Eggleton BJ, et al. Integrated sources of photon quantum states based on nonlinear optics. Light Sci Appl. 2017;6:e17100.
[5] Alibart O, D'Auria V, De Micheli M, et al. Quantum photonics at telecom wavelengths based on lithium niobate waveguides. J Opt. 2016;18:104001.
[6] Arizmendi L. Photonic applications of lithium niobate crystals. Phys Stat Sol. 2004;201:253–283.
[7] Pohl A. A review of wireless SAW sensors. IEEE Trans. Ultrason. Ferroelectr. Freq. Control. 2000;47: 317–332.
[8] Boes A, Corcoran B, Chang L, et al. Status and potential of lithium niobate on insulator (LNOI) for photonic integrated circuits. Lasers Photonics Rev. 2018;1700256:
[9] Honardoost A, Abdelsalam K, Fathpour S. Rejuvenating a versatile photonic material: thin-film lithium niobate. Lasers Photonics Rev. 2020;14:2000088.
[10] Chen JY, Sua YM, Ma ZH, et al. Efficient parametric frequency conversion in lithium niobate nanophotonic chips. OSA Contin. 2019;2:2914–2924.
[11] Poberaj G, Hu H, Sohler W, et al. Lithium niobate on insulator (LNOI) for micro-photonic devices. Laser Photon Rev. 2012;6:488–503.
[12] Luke K, Kharel P, Reimer C, et al. Wafer-scale low-loss lithium niobate photonic integrated circuits. Opt Express. 2020;28:24452–24458.

[13] Wang C, Burek MJ, Lin Z, et al. Integrated high quality factor lithium niobate microdisk resonators. Opt Express. 2014;22:30924–30933.
[14] Lin J, Xu Y, Fang Z, et al. Fabrication of high-Q lithium niobate microresonators using femtosecond laser micromachining. Sci Rep. 2015;5:8072.
[15] Wu R, Wang M, Xu J, et al. Long low-loss-lithium niobate on insulator waveguides with sub-nanometer surface roughness. Nanomaterials. 2018;8:910.
[16] Zhang M, Wang C, Cheng R, et al. Monolithic ultra-high-Q lithium niobate microring resonator. Optica. 2017;4:1536–1537.
[17] Zhou J, Gao R, Lin J, et al. Electro-optically switchable optical true delay lines of meter-scale lengths fabricated on lithium niobate on insulator using photolithography assisted chemo-mechanical etching. Chin Phys Lett. 2020;37:084201.
[18] Wu R, Zhang J, Yao N, et al. Lithium niobate micro-disk resonators of quality factors above $10^7$. Opt Lett. 2018;43:4116–4119.
[19] Qi Y, Li Y. Integrated lithium niobate photonics. Nanophotonics. 2020;9:1287–1320.
[20] Lin J, Bo F, Cheng Y, et al. Advances in on-chip photonic devices based on lithium niobate on insulator. Photonics Res. 2020;8:1910-1936.
[21] Kong Y, Bo F, Wang W, et al. Recent progress in lithium niobate: optical damage, defect simulation, and on-chip devices. Adv Mater. 2019;32:1806452.
[22] Luo R, He Y, Liang H, et al. Highly tunable efficient second-harmonic generation in a lithium niobate nanophotonic waveguide. Optica. 2018;5:1006–1011.
[23] Luo R, He Y, Liang H, et al. Semi-nonlinear nanophotonic waveguides for highly efficient second-harmonic generation. Laser Photon Rev. 2019;13:1800288.
[24] Wang C, Langrock C, Marandi A, et al. Ultrahigh-efficiency wavelength conversion in nanophotonic periodically poled lithium niobate waveguides. Optica. 2018;5:1438–1441.
[25] Ito H, Takyu C, Inaba H. Fabrication of periodic domain grating in LiNbO3 by electron beam writing for application of nonlinear optical processes. Electron Lett. 1991;27:1221–1222.
[26] Mohageg M, Strekalov DV, Savchenkov AA, et al. Calligraphic poling of Lithium Niobate. Opt Express. 2005;13:3408–3419.
[27] Ya. V, Shur AR, Akhmatkhanov IS. Baturin. Micro- and nano-domain engineering in lithium niobate. Appl Phys Rev. 2015;2:040604.
[28] Chen X, Karpinski P, Shvedov V, et al. Quasi-phase matching via femtosecond laser-induced domain inversion in lithium niobate waveguides. Opt Lett. 2016;41:2410–2413.
[29] Hao Z, Zhang L, Mao W, et al. Second-harmonic generation using d 33 in periodically poled lithium niobate microdisk resonators. Photonics Res. 2020;8:311–317.
[30] Wang C, Xiong X, Andrade N, et al. Second harmonic generation in nano-structured thin-film lithium niobate waveguides. Opt Express. 2017;25:6963–6973.
[31] Rao A, Chiles J, Khan S, et al. Second-harmonic generation in single-mode integrated waveguides based on mode-shape modulation. Appl Phys Lett. 2017;110:111109.
[32] Wang C, Li Z, Kim M-H, et al. Metasurface-assisted phase-matching-free second harmonic generation in lithium niobate waveguides. Nat Commun. 2017;8:2098.
[33] Fedotova A, Younesi M, Sautter J, et al. Second-harmonic generation in resonant nonlinear metasurfaces based on lithium niobate. Nano Lett. 2020;20:8608–8614.
[34] Carletti L, Li C, Sautter J, et al. Second harmonic generation in monolithic lithium niobate metasurfaces. Opt Express. 2019;27:33391–33398.
[35] Fang B, Li H, Zhu S, et al. Second-harmonic generation and manipulation in lithium niobate slab waveguides by grating metasurfaces. Photonics Res. 2020;8:1296–1300.

[36] Ge L, Chen Y, Jiang H, et al. Broadband quasi-phase matching in a MgO:PPLN thin film. Photonics Res. 2018;6:954–958.
[37] Liu S, Zheng Y, Chen X. Cascading second-order nonlinear processes in a lithium niobate-on-insulator microdisk. Opt Lett. 2017;42:3626–3629.
[38] Lin J, Yao N, Hao Z, et al. Broadband quasi-phase-matched harmonic generation in an on-chip monocrystalline lithium niobate microdisk resonator. Phys Rev Lett. 2019;122:173903.
[39] Hao Z, Zhang L, Gao A, et al. Periodically poled lithium niobate whispering gallery mode microcavities on a chip. Sci. China-Phys. Mech. Astron. 2018;61:114211.
[40] Zhang L, Hao Z, Luo Q, et al. Dual-periodically poled lithium niobate microcavities supporting multiple coupled parametric processes. Opt Lett. 2020;45:3353–3356.
[41] Chen J-Y, Ma Z-H, Sua YM, et al. Ultra-efficient frequency conversion in quasi-phase-matched lithium niobate microrings. Optica. 2019;6:1244–1245.
[42] Lu J, Surya JB, Liu X, et al. Periodically poled thin-film lithium niobate microring resonators with a second-harmonic generation efficiency of 250,000%/W. Optica. 2019;6:1455–1460.
[43] Lu J, Li M, Zou C-L, et al. Toward 1% single-photon anharmonicity with periodically poled lithium niobate microring resonators. Optica. 2020;7:1654–1659.
[44] Diziaina S, Geiss R, Zilk M, et al. Second harmonic generation in free-standing lithium niobate photonic crystal L3 cavity. Appl Phys Lett. 2013;103:
[45] Li Y, Wang C, Lončar M. Design of nano-groove photonic crystal cavities in lithium niobate. Opt Lett. 2015;40:2902–2905.
[46] Jiang H, Yan X, Liang H, et al. High harmonic optomechanical oscillations in the lithium niobate photonic crystal nanocavity. Appl Phys Lett. 2020;117:081102.
[47] Jiang H, Liang H, Luo R, et al. Nonlinear frequency conversion in one dimensional lithium niobate photonic crystal nanocavities. Appl Phys Lett. 2018;113:
[48] Li M, Liang H, Luo R, et al. High-Q 2D lithium niobate photonic crystal slab nanoresonators. Laser & Photonics Reviews 2019;13:1800228.
[49] Hao Z, Wang J, Ma S, et al. Sum-frequency generation in on-chip lithium niobate microdisk resonators. Photonics Res. 2017;5:623–628.
[50] Ye X, Liu S, Chen Y, et al. Sum-frequency generation in lithium-niobate-on-insulator microdisk via modal phase matching. Opt Lett. 2020;45:523–526.
[51] Li G, Chen Y, Jiang H, et al. Broadband sum-frequency generation using $d_{33}$ in periodically poled $LiNbO_3$ thin film in the telecommunications band. Opt Lett. 2017;42:939–942.
[52] Rueda A, Sedlmeir F, Collodo MC, et al. Efficient microwave to optical photon conversion: an electro-optical realization. Optica. 2016;3:597–604.
[53] Shao L, Yu M, Maity S, et al. Microwave-to-optical conversion using lithium niobate thin-film acoustic resonators. Optica. 2019;6:1498–1505.
[54] Shao L, Sinclair N, Leatham J, et al. Integrated microwave acousto-optic frequency shifter on thin-film lithium niobate. Opt Express. 2020;28:23728–23738.
[55] Kaufmann F, Sergeyev A, Escalé MR, et al. On-Chip Optical Parametric Amplification in Subwavelength Lithium Niobate Nanowaveguides. in Advanced Photonics 2018 (BGPP, IPR, NP, NOMA, Sensors, Networks, SPPCom, SOF), OSA Technical Digest (online) (Optical Society of America, 2018), paper JTu5A.52.
[56] Chen J, Sua YM, Ma Z, et al. Phase-sensitive Amplification in Nanophotonic Periodically Poled Lithium Niobate Waveguides. in Conference on Lasers and Electro-Optics, OSA Technical Digest (Optical Society of America, 2020), paper SM3L.5.

[57] Bruch AW, Liu X, Surya JB, et al. On-chip $\chi^{(2)}$ microring optical parametric oscillator. Optica. 2019;6:1361–1366.
[58] Canalias C, Pasiskevicius V. Mirrorless optical parametric oscillator. Nature Photon. 2007;1:459–462.
[59] Liljestrand C, Zukauskas A, Pasiskevicius V, et al. Highly efficient mirrorless optical parametric oscillator pumped by nanosecond pulses. Opt Lett. 2017;42:2435–2438.
[60] Jin H, Liu FM, Xu P, et al. On-chip generation and manipulation of entangled photons based on reconfigurable lithium-niobate waveguide circuits. Phys Rev Lett. 2014;113:103601.
[61] Luo R, Jiang H, Rogers S, et al. On-chip second-harmonic generation and broadband parametric down-conversion in a lithium niobate microresonator. Opt Express. 2017;25:24531–24539.
[62] Zhao J, Ma C, Rüsing M, et al. High quality entangled photon pair generation in periodically poled thin-film lithium niobate waveguides. Phys Rev Lett. 2020;124:163603.
[63] Ma Z, Chen J-Y, Li Z, et al. Ultrabright quantum photon sources on chip. Phys Rev Lett. 2020;125:263602.
[64] Nagy JT, Reano RM. Submicrometer periodic poling of lithium niobate thin films with bipolar preconditioning pulses. Opt Mater Express. 2020;10:1911–1920.
[65] Luo K-H, Ansari V, Massaro M, et al. Counter-propagating photon pair generation in a nonlinear waveguide. Opt Express. 2020;28:3215–3225.
[66] Wolf R, Breunig I, Zappe H, et al. Cascaded second-order optical nonlinearities in on-chip micro rings. Opt Express. 2017;25:29927–29933.
[67] Wang M, Yao N, Wu R, et al. Strong nonlinear optics in on-chip coupled lithium niobate microdisk photonic molecules. New J Phys. 2020;22:073030.
[68] Liu S, Zheng Y, Fang Z, et al. Effective four-wave mixing in the lithium niobate on insulator microdisk by cascading quadratic processes. Opt Lett. 2019;44:1456–1459.
[69] Hickstein DD, Carlson DR, Kowligy A, et al. High-harmonic generation in periodically poled waveguides. Optica. 2017;4:1538–1544.
[70] Ding T, Zheng Y, Chen X. Integration of cascaded electro-optic and nonlinear processes on a lithium niobate on insulator chip. Opt Lett. 2019;44:1524–1527.
[71] Newbury N. Searching for applications with a fine-tooth comb. Nat Photon. 2011;5:186–188.
[72] Coddington I, Newbury N, Swann W. Dual-comb spectroscopy. Optica. 2016;3:414–426.
[73] Marin-Palomo P, Kemal JN, Karpov M, et al. Microresonator-based solitons for massively parallel coherent optical communications. Nature. 2017;546:274–279.
[74] Trocha P, Karpov M, Ganin D, et al. Ultrafast optical ranging using microresonator soliton frequency combs. Science. 2018;359:887–891.
[75] Wang C, Zhang M, Yu M, et al. Monolithic lithium niobate photonic circuits for Kerr frequency comb generation and modulation. Nat Commun. 2019;10:978.
[76] He Y, Yang Q-F, Ling J, et al. Self-starting bi-chromatic $LiNbO_3$soliton microcomb. Optica. 2019;6:1138–1144.
[77] Gong Z, Liu X, Xu Y, et al. Soliton microcomb generation at 2 μm in *z*-cut lithium niobate microring resonators. Opt Lett. 2019;44:3182–3185.
[78] Gong Z, Liu X, Xu Y, et al. Near-octave lithium niobate soliton microcomb. Optica. 2020;7:1275–1278.
[79] Kippenberg TJ, Gaeta AL, Lipson M, et al. Dissipative Kerr solitons in optical microresonators. Science. 2018;361:eaan8083.

[80] Kues M, Reimer C, Lukens JM, et al. Quantum optical microcombs. Nat Photonics. 2019;13:170–179.
[81] Zhang M, Buscaino B, Wang C, et al. Broadband electro-optic frequency comb generation in a lithium niobate microring resonator. Nature. 2019;568:373–377.
[82] Dudley JM, Genty G, Coen S. Supercontinuum generation in photonic crystal fiber. Rev Mod Phys. 2006;78:1135.
[83] Lu J, Surya JB, Liu X, et al. Octave-spanning supercontinuum generation in nanoscale lithium niobate waveguides. Opt Lett. 2019;44:1492–1495.
[84] Yu M, Desiatov B, Okawachi Y, et al. Coherent two-octave-spanning supercontinuum generation in lithium-niobate waveguides. Opt Lett. 2019;44:1222–1225.
[85] Jankowski M, Langrock C, Desiatov B, et al. Ultrabroadband nonlinear optics in nanophotonic periodically poled lithium niobate waveguides. Optica. 2020;7:40–46.
[86] Yu M, Okawachi Y, Cheng R, et al. Raman lasing and soliton mode-locking in lithium niobate microresonators. Light Sci Appl. 2020;9:9.
[87] Cai L, Mahmoud A, Khan M, et al. Acousto-optical modulation of thin film lithium niobate waveguide devices. Photonics Res. 2019;7:1003–1013.
[88] Lan S, Kang L, Schoen DT, et al. Backward phase-matching for nonlinear optical generation in negative-index materials. Nat Mater. 2015;14:807–811.
[89] Duan J-C, Zhang J-N, Zhu Y-J, et al. Generation of narrowband counterpropagating polarization-entangled photon pairs based on thin-film lithium niobate on insulator. J Opt Soc Am B. 2020;37:2139–2145.
[90] Szabados J, Puzyrev DN, Minet Y, et al. Frequency comb generation via cascaded second-order nonlinearities in microresonators. Phys Rev Lett. 2020;124:203902.
[91] Yuan L, Lin Q, Xiao M, et al. Synthetic dimension in photonics. Optica. 2018;5:1396–1405.
[92] Yuan L, Dutt A, Qin M, et al. Creating locally interacting Hamiltonians in the synthetic frequency dimension for photons. Photonics Res. 2020;8:B8–B14.
[93] Li G, Zheng Y, Dutt A, et al. Dynamic band structure measurement in the synthetic space. Sci Adv. 2021;7:eabe4335.
[94] Wang S, Yang L, Cheng R, et al. Incorporation of erbium ions into thin-film lithium niobate integrated photonics. Appl. Phys. Lett. 2020;116:151103.
[95] Liu Y, Yan X, Wu J, et al. On-chip erbium-doped lithium niobate microcavity laser. Sci. China Phys. Mech. Astron. 2021;64:234262.
[96] Desiatov B, Lončar M. Silicon photodetector for integrated lithium niobate photonic. Appl Phys Lett. 2019;115:121108.